Available online at www.sciencedirect.com

ScienceDirect

Physica C 468 (2008) 669–673

PHYSICA C

www.elsevier.com/locate/physc

Quantum oscillation of the *c*-axis resistivity due to entrance of pancake vortices into micro-fabricated $Bi_2Sr_2CaCu_2O_{8+\delta}$ intrinsic Josephson junctions

I. Kakeya *, K. Fukui, K. Kawamata, T. Yamamoto, K. Kadowaki

Institute of Materials Science, University of Tsukuba, 1-1-1 Ten-nodai, Tsukuba, Ibaraki 305-8573, Japan

Accepted 30 November 2007
Available online 29 February 2008

Abstract

The *c*-axis resistance in $Bi_2Sr_2CaCu_2O_{8+\delta}$ intrinsic Josephson junctions (IJJs) with areas of the *ab*-plane less than 2 μm^2 were measured as functions of applied magnetic field and angle to the crystalline axes. When the magnetic field is tilted off from the lock-in state of Josephson vortices, several sharp dips are found. The separation between the dips approaches to the value corresponding to ϕ_0 with further tilting the external magnetic field. This behavior is attributed to the penetration of a quantized pancake vortex into the tiny IJJ. This argument is further supported by the result that the *c*-axis resistance under magnetic fields parallel to the *c*-axis shows identical stepwise behavior.

PACS: 74.25.−q; 74.72.Hs; 74.78.Na

Keywords: Intrinsic Josephson junction; Josephson vortex; Flux quantization; Penetration depth; Mesoscopic superconductors

1. Introduction

It has been known that flux begins to penetrate into a type II superconductor as a quantized vortex ϕ_0 just above the lower critical field H_{c1}. This was firstly demonstrated by historical experiments by Doll and Näbauer [1] and Deaver and Fairbank [2]. The Little–Parks effect [3,4], oscillation of the critical temperature T_c of superconductors with tiny halls is one of the most beautiful evidences of the flux quantization. In high-T_c superconductors, the Little–Parks effect was firstly claimed in $YBa_2Cu_3O_{7-\delta}$ thin films patterned with the focused ion beam (FIB) method [5].

Quite recently, several oscillating phenomena attributed to the flux quantization have been investigated on Josephson vortices (JVs) which are induced by magnetic field parallel to the *ab*-plane of $Bi_2Sr_2CaCu_2O_{8+\delta}$ (Bi2212) intrinsic Josephson junctions (IJJ) with widths of less than 50 μm. The *c*-axis resistance as a function of magnetic field oscillates with a period of the field inducing a half or one ϕ_0 in a Josephson junction stacking along the *c*-axis [6–10]. In narrower junctions with respect to the external magnetic field, oscillation of the critical current $J_c(H)$ and Fiske step in current–voltage (*I*–*V*) characteristics along the *c*-axis were also reported by several authors [11–13]. These phenomena are not the results of penetrations of a single vortex but mainly attributed to the intrinsic pinning [14] which confines JVs into block layers and restricts their arrangements one dimensionally along the layers.

Moreover, interaction between JVs and pancake vortices (PVs) has also been an interesting issue in IJJ. Variety of phases have been predicted theoretically [15] and observed by couple of imaging techniques [16,17]. Although such imaging techniques have a great advantage that arrangements of vortices can be revealed without an ambiguity, it is difficult to obtain thermodynamic changes

---

* Corresponding author. Present address: Department of Electronic Science and Engineering, Kyoto University Kyotodaigaku-Katsura, Nishikyo-ku, Kyoto 615-8510, Japan.

E-mail address: kakeya@kuee.kyoto-u.ac.jp (I. Kakeya).

0921-4534/$ - see front matter © 2008 Elsevier B.V. All rights reserved.
doi:10.1016/j.physc.2007.11.064

of sample quantitatively and to use at high magnetic fields. Transport measurements in samples with a few JVs and PVs allow us to estimate thermodynamic properties of the interaction between two types of vortices and various vortex phases.

This paper reports on oscillating or stepwise behavior of the *c*-axis resistance in IJJs with areas of the *ab*-plane (superconducting electrodes) less than 2 µm^2. This phenomenon is interpreted to be attributed to penetration of quantized vortices one-by-one. The results enable us to estimate the penetration depth for the *ab*-plane λ_{ab} as a function of magnetic field and lower critical field H_{c1} without complicated assumptions.

2. Experimental

Bi2212 sub-micron junctions were fabricated by the FIB machine SMI2050 as shown in Fig. 1. This method is based on the technique invented by Kim et al. [18]. In advance of the fabrication, a single crystal glued on a MgO substrate was cleaved with Scotch adhesive tapes and the fresh surface was immediately covered by evaporated silver (gold) with a shadow mask which makes four electrodes. We had prepared samples listed in Table 1 and an image of a junction is shown in Fig. 2.

Measurements of the *c*-axis resistivity ρ_c were done with the four-probe method with either DC or AC bias. Voltage between the electrodes is considered to be equivalent to the voltage along the junction because current supplied with the current electrodes is concentrated within the small cross-section $A = L \times W$. For AC measurement, the SR850 lock-in amplifier was employed and the excitation current was sinusoidal with frequencies being 17 and 31 Hz. External magnetic field was applied by a split-pair superconducting magnet and the samples were rotated by a precise goniometer in fixed horizontal magnetic fields. Angle θ is measured from the *ab*-plane as seen in Fig. 1d.

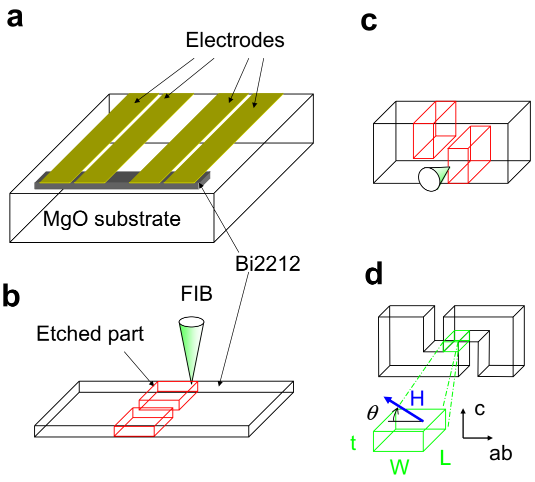

Fig. 1. (a) Sample before the fabrication. Width, thickness, and length of the crystals are ~100 µm, ~10 µm, $\gtrsim$ 2 mm, respectively. (b) Etching from the top. Red contours are etched to reduce the width. (c) Lateral etching for the reduced part. Two gaps from the top and the bottom are formed so as to overlap along the *c*-axis. (d) Finished shape and correspondence *L*, *W*, and *t* against the external field direction. (For interpretation of the references to colour in this figure legend, the reader is referred to the web version of this article.)

Table 1
List of samples

	$L \times W \times t$ (µm^3)	ϕ_0/A (G)	T_c (K)
#40	1.10 × 1.13 × 0.25	17	84
#42	1.53 × 1.45 × 0.26	9.3	86
#46	0.80 × 2.06 × 0.51	13	87

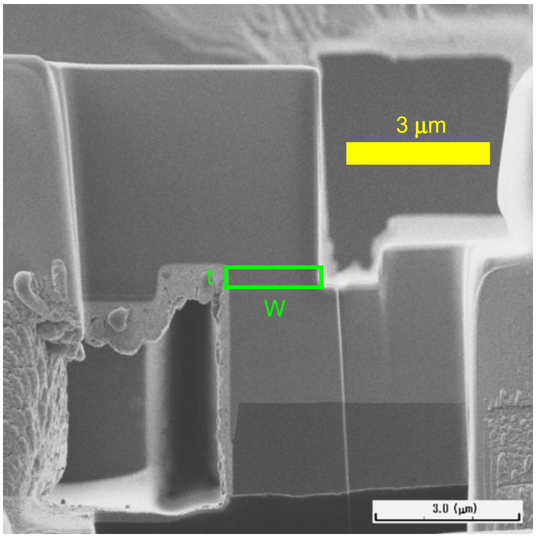

Fig. 2. Lateral image of #44. Measured resistance is from coutoured part.

3. Results and discussion

Fig. 3 represents $\rho_c - \theta$ curve in sample #42 for various external magnetic fields. In data above 4 kOe, one finds

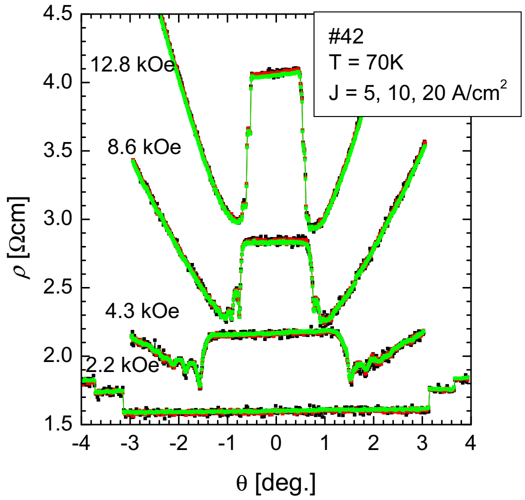

Fig. 3. Angular dependence of the *c*-axis resistance of #42.